ANN based speed control of switched reluctance motor using MATLAB-interfaced DSP controller

Veena Wilson[1,2], Latha Padinjaredath Govindan[1]
[1]School of Engineering, Cochin University of Science and Technology, Kochi, Kerala, India
[2]Department of Electrical Engineering, Federal Institute of Science and Technology, Ernakulam, India

Article Info

ABSTRACT

The switched reluctance motor (SRM) is gaining significance as a competitive motor in industries due to its prominent features such as absence of rare-earth elements, strong fault tolerance, and competitive efficiency. This paper presents a comprehensive framework to a novel and simplified hardware implementation of SRM drive, accompanied by a stepwise procedure to develop the control process that includes system modelling with simulation analysis and experimental validation, useful for the novice researchers. A precise hardware control environment is introduced, by integrating MATLAB/Simulink platform with digital signal processor (DSP) microcontroller - TMS320F280049C, which minimizes the complexities of traditional controller coding. The paper provides an in-depth explanation of deployment of artificial neural network (ANN) speed control block, offering valuable insights into the practical aspects of ANN-based control in MATLAB. The paper also compares closed-loop speed control using proportional-integral (PI) and ANN control in SRM, and the results demonstrate accurate and adaptive performance of ANN control for variable speed- load conditions.

Corresponding Author:

Veena Wilson
School of Engineering, Cochin University of Science & Technology
Kochi, Kerala, India
Email: veenawilson@cusat.ac.in

1. INTRODUCTION

Switched reluctance motors (SRMs) are witnessing growing popularity over the past decades owing to the unique properties of these machines, which align well with the growing demand for efficient, reliable, and sustainable electric motors across various industries. SRMs feature a simple, rugged structure and exhibit excellent fault tolerance making them highly reliable and durable, which is crucial for many industrial and automotive applications [1]. While traditional permanent magnet synchronous motors (PMSMs) have to rely on rare earth materials, SRMs operate without these magnets [2]. The ability of SRMs to perform efficiently over a wide range of speeds makes them ideal for use in electric vehicles and industries requiring variable-speed motors [3]. Its high torque density and efficiency align with the push towards sustainable transportation. As issues like vibration and acoustic noise are gradually mitigated through advanced control techniques, SRMs are becoming more viable for broader applications [4]. The SRM's alignment with the demands of modern industries viz. cost-effectiveness, environmental sustainability, and advanced control capabilities, makes it a critical technology in the evolving landscape of electric motors.

Various control strategies have been investigated for performance improved implementation of SRM, including fuzzy control [5], finite-time proportional control [6], improved dynamics PI control [7], adaptive supervisory self-learning control [8], feedforward-trained ANN control [9], digital control [10], and

robust speed control [11]. However, these studies offer only partial transient performance improvements with complex implementation procedures providing only limited insights into hardware implementation aspects.

The development history of hardware controllers for SRMs has spanned several decades and has utilized a variety of platforms, such as programmable logic controllers (PLCs) [12], field-programmable gate arrays (FPGAs) [13], and specialized microcontroller-based platforms like STM32 [14], [15] and TMS320 [10]. In this evolution, the Texas Instruments' TMS320 series of digital signal processors (DSPs) continued to evolve as the best controllers that offer features like advanced PWM control, real-time processing and high-speed feedback loops, which are crucial for implementing fine-grained control strategies. They have proved its efficiency in designing effective proportional-integral (PI) type controllers and Model Predictive Controllers for photovoltaic systems and power electronic converters [16], [17]. It has been proven efficient for ANN-based control of five-level inverters which ensure selective harmonic elimination [18]. TI C2000 DSPs offer a practical and simple control design for DC motors [19]. The C2000 TMS320F28388D has been used to develop a control platform for a parameter estimation method in induction motors (IMs) [20].

Although the use of DSP microcontrollers has been widely adopted in research and well discussed in the literature, they come with a lot of complicated algorithms and codes for the implementation, which can be time-consuming and challenging to implement, particularly for researchers unfamiliar with the coding environment [10]. In this context, using TI C2000 DSPs with MATLAB offers a practical way to turn models into hardware, linking academic research, embedded system design, and real-world applications [21]. The use of MATLAB/Simulink Embedded Coder tools, without manual coding, offers time and cost efficiency, accelerates execution, and is highly effective for both research and industrial control applications [22]. The Embedded Coder generates the code automatically, reducing the time needed for solving the problems of long development cycles and complicated programming for traditional embedded system design. MATLAB Simulink environment can also be used for real-time simulation of power electronic systems [23], [24]. The implementation of the closed-loop v/f control algorithm of IM in real time using MATLAB/Simulink Embedded Coder with TMS320F28335 DSP proves the accessibility and cost-effectiveness of DSP programming for a broader range of users [21].

While TI C2000 DSPs, such as the TMS320F280049C, offer significant potential, the literature provides limited structured guidance for their use in SRM operations. This gap makes real-time deployment challenging for novice researchers. The existing SRM control studies often lack comprehensive solutions that address both improved transient response and practical hardware implementation. Furthermore, there are no prior works presenting a MATLAB-integrated DSP-based methodology with a clear, step-by-step hardware implementation of SRM. Comparative evaluations of PI and ANN controllers also remain insufficiently explored, particularly concerning real-time performance and ease of implementation. Thus, the proposed work is an attempt to address the above issues with the following major contributions: i) A detailed step-by-step hardware implementation methodology for SRM, aimed at simplifying deployment for novice researchers; ii) A simplified MATLAB/Simulink based implementation of hardware control, eliminating the need for complex DSP coding; and iii) An efficient ANN control topology and its hardware implementation demonstrating improved transient performance compared with the PI controllers.

The organization of the work is as outlined: i) Section 2 explains the functioning of the SRM drive along with the building of a MATLAB model using finite element analysis (FEA); ii) The working of SRM with MATLAB-interfaced microcontroller is presented in section 3; iii) The fourth section focuses on the implementation of the speed controller using ANN; iv) While section 5 reports experimental results and evaluation; and v) Lastly, the final conclusion offers a summary of findings and observations presented in the paper.

2. SRM DRIVE SYSTEM AND SIMULATION ANALYSIS

SRMs are designed with a simple construction, featuring projected stator and rotor poles. Among the many converter topologies explored, the asymmetric half bridge converter proved to be the most prevalent power converter for SRM drives [25]-[27]. Different phases of SRM are excited in a sequential manner to develop a continuous torque in the motor. Figure 1 provides an illustration of the entire hardware setup. The asymmetric half-bridge converter receives gate pulses from the controller and according to the rotor position acquired from quadrature encoder pulse (QEP) encoder, the converter excites the phases of the motor in a sequential manner. The motor is coupled with a loading system equipped with a spring balance arrangement.

A simulation analysis of SRM under study is conducted for analyzing the conduction window corresponding to the maximum torque as well as the approximate P and I gain. The simulation model is developed with an electrical block, mechanical block, PI controller block as well as voltage signal generation block. The electrical block is modelled using (1)-(3) [10], [25]:

$$V = iR + \frac{d\lambda(\theta,i)}{dt} \qquad (1)$$

$$\lambda(\theta,i) = \int_0^t (V - iR)\,dt \qquad (2)$$

$$i = \frac{\lambda(\theta,i)}{L(\theta,i)} \qquad (3)$$

where i, V, R, L and λ correspond to phase- current, voltage, resistance, inductance and flux linkage of each phase and θ represents rotor position. Mechanical block of the SRM is modelled using the (4).

$$T_e = J\frac{d\omega}{dt} + B\omega + T_L \qquad (4)$$

Here, J, B, ω, T_L and T_e, represent the rotational inertia, viscous friction, speed, load and developed torque respectively. FEA of the machine under study is performed to determine inductance and torque and profiles for different rotor positions and current, and are used for modelling the SRM. Block diagram representation of the SRM for simulation in MATLAB environment is as given by Figure 2(a). Figures 2(b) and 2(c) illustrates a 3D plot of the L-profile showing unaligned /aligned inductance values (L_u/L_a) and 2D torque plot respectively. From torque profile, it is inferred that the maximum torque generation happens in the conduction window of 3°-21°.The P and I gain values are configured using iterative method and is found to be 0.0085 and 0.085 respectively. In SRM drives, the commonly used hysteresis control causes variable switching frequency issues that hinder digital deployment, but applying PI controllers with single-pulse control reduces the frequency to its fundamental value, achieving lower current ripple and improved torque-per-ampere [10], [28]. Here, the machine speed is regulated by varying the turn on angle with the help of a PI controller which is one of the simplest and most commonly used control strategies in SRM speed control. Accurate energization of the SRM at specific angles is necessary to ensure the required torque production under the intended load conditions [29].
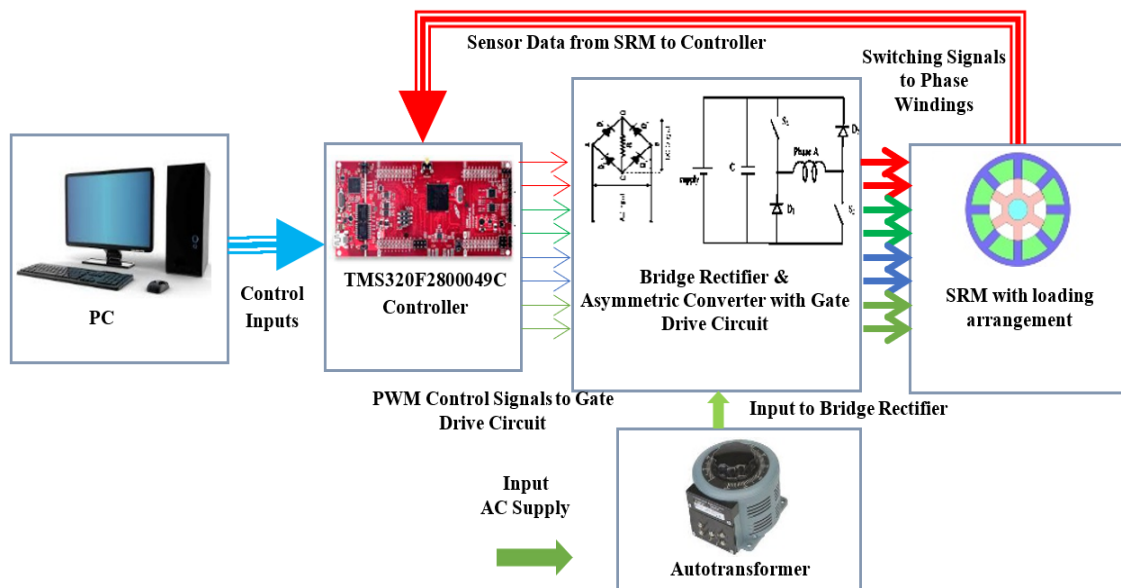

Figure 1. Illustration of the developed SRM drive system

Voltage pulses are generated using the MATLAB function block. Figures 3(a) and 3(b) depict the speed control for different test speeds (500, 800, 600, and 700 rpm) at test time instants (0, 40, 60, and 80 seconds, respectively) and the corresponding turn-on angle variation at no load condition with the PI controller. The model is simulated with a load of 1.8 Nm, and Figures 4(a) and 4(b) represent the corresponding phase current, voltage, and inductance profiles at 800 rpm and average torque waveform for the above speeds, respectively. The outcomes of the simulation confirm the robustness of the controller, maintaining accurate speed tracking and stable torque production with adaptive turn-on angle adjustment under dynamic conditions.
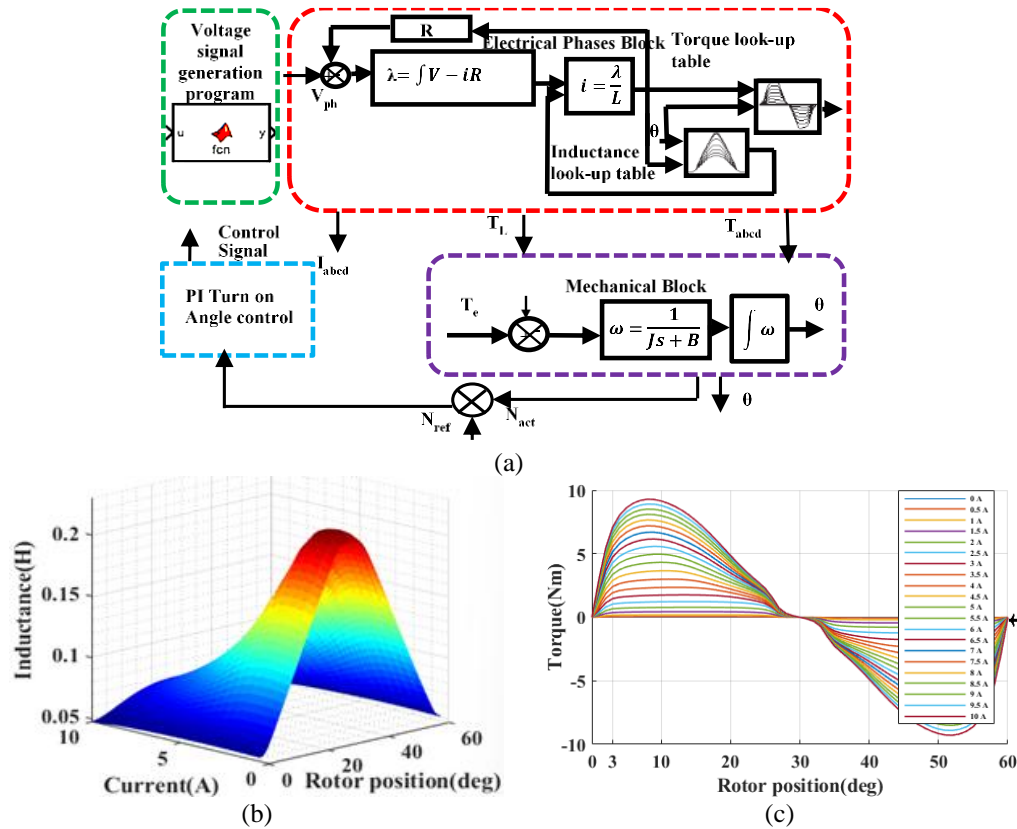
(a)

(b)

(c)

Figure 2. Simulation model and characteristic of SRM: (a) block diagram, (b) L-θ profile, and (c) T_e- i- θ profile
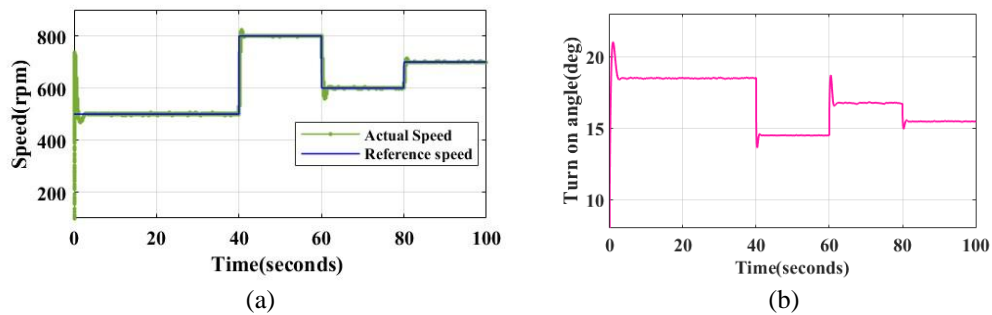

(a)

(b)

Figure 3. Speed regulation characteristics of SRM under no-load condition using PI controller:
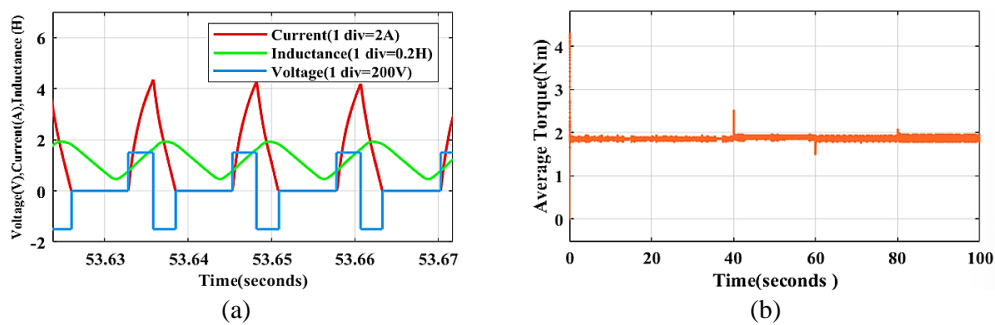(a) closed loop speed response and (b) turn on angle variation for test speeds

(a)

(b)

Figure 4. Electrical and torque characteristics of the SRM: (a) phase voltage, current, and inductance
waveforms at 800 rpm and (b) average developed torque of 1.8 Nm at specified test conditions

3.   IMPLEMENTATION OF MATLAB INTEGRATED DSP CONTROL

The combination of high performance, integrated features, development tools, and reliability makes Texas Instruments (TI) microcontrollers an excellent choice for SRM speed control [30]. The control logic producing the gate pulses is implemented using the TI microcontroller TMS320F280049C, integrated with MATLAB [31]-[33]. The process of converting MATLAB/Simulink models into executable programs for microcontrollers involves several stages, which utilize tools like MATLAB, Simulink, and Embedded Coder, integrating with development environments such as Code Composer Studio and Control SUITE. The implementation of the control logic in the hardware setup is displayed in a sequential manner as shown in Figure 5. Once it is ensured that the above software packages and supports are installed, then the hardware implementation of SRM is initiated with the following stages.
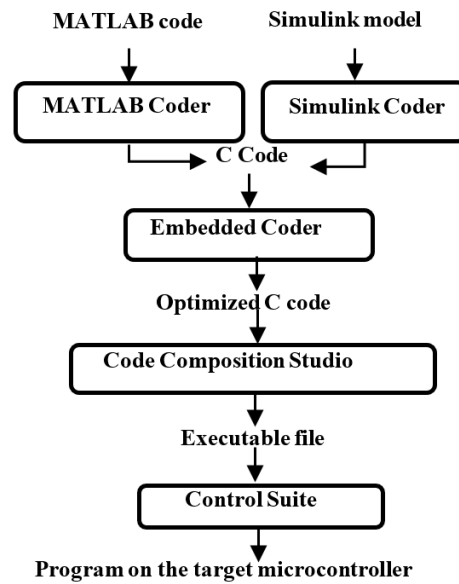

Figure 5. MATLAB interfacing with DSP controller

3.1. Pulse generation control logic

Initially, a simple control logic is developed setting a ramp signal instead of rotor position and the pulses are generated as given by Figure 6(a). GPIO blocks available in the C2000 microcontroller block sets are used to output four gate pulses representing four phases to the respective pins of the microcontroller. In the next stage, a QEP sensor with 4096 ppr resolution is used for position sensing. It has two quadrature channel pulses (A & B), producing 1024 pulses per revolution and a quadrature index pulse which indicates the reference point of the encoder for detecting a complete revolution. The quadrature and index pulses obtained from the QEP encoder are as presented in Figure 6(b).
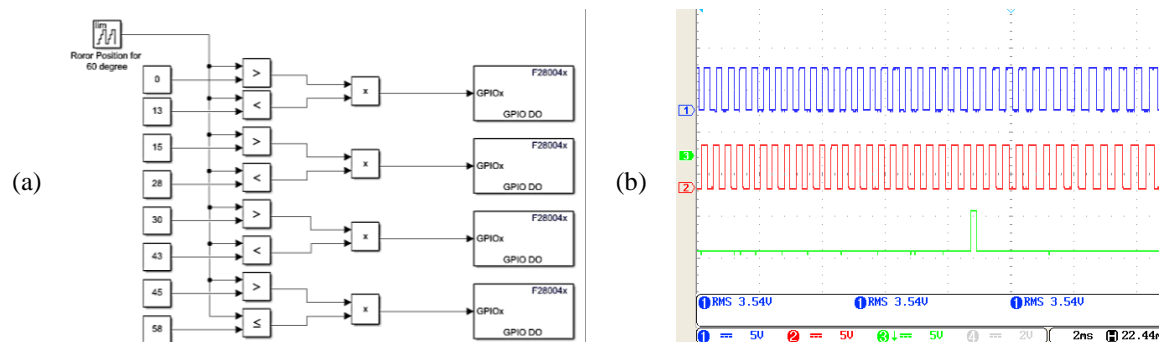

Figure 6. Pulse signal generation and encoder feedback used in SRM control: (a) MATLAB pulse generation blocks and (b) QEP encoder pulses (A, B and index pulse)

Using eQEP block in MATLAB, real time position count is obtained which is then used for pulse generation [34]. This increasing count value is converted to 60° and is used for gate pulse generation. Pulse generation logic using eQEP block, as well as the output pulse with position ramp signal through digital to analog converter block are demonstrated in Figures 7(a) and 7(b). Once the correct pulse generation is achieved, the SRM motor is made to rotate by providing 8 gate pulses to the 4-phase converter.

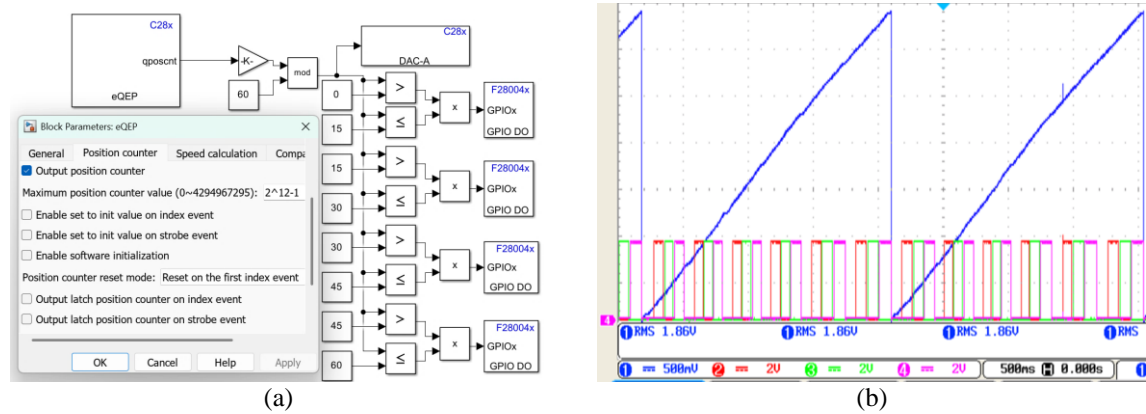(a)   (b)

Figure 7. Pulse generation mechanism based on encoder feedback for SRM control: (a) pulse generation logic using eQEP block and (b) output pulses and position ramp signals

3.2. Starting and real time speed monitoring of SRM

For starting SRM, an initial ramp signal is given as the position signal and the phases are excited in a sequential manner. The rotor slowly catches the excited stator poles and once the index position is reached, then rotor position is reset, after which the phase having lowest inductance value is excited first. This is followed by an excitation sequence so that the rotor will be rotated in anticlockwise direction. Here, the phase (phase C) which is having lowest inductance value next to the index position is exited first and the phases are excited in the sequence C-D-A-B-C, giving a continuous torque for the motor. For the instantaneous speed calculation, the same eQEP block is used with speed calculation tab. The timer pre-scaler values are set and the (5) is used to calculate the real-time speed.

$$\text{Speed in rpm} = \frac{\text{Distance (upevents) for one revoultion}}{\text{Time taken(seconds) for one revolution}} \times 60 = \frac{1}{QCPRD \times 4096 \times eCTP/F_{sys}} \times 60 \tag{5}$$

Here $QCPRD$, $eCTP$ and F_{sys} represents quadrature capture period register, enhanced capture timer period, and system clock frequency respectively.

3.3. Offset and conduction window analysis

For an 8/6 SRM, the inductance profile will be repeating for every 60° [25], [32]. Excitation should be applied during the positive torque region to ensure the generation of motoring torque. The torque developed, T_e is given by the (6), where $i, \frac{dL}{d\theta}$ represent current and inductance change with angle respectively.

$$T_e = \frac{1}{2} i^2 \frac{dL}{d\theta} \tag{6}$$

Inductance profiles of all the phases are plotted measuring inductance under static condition. Analyzing the inductance profiles, the phase with minimum inductance next to the index position is found to have an offset of 10° from the zero value of rotor position. To determine conduction window corresponding to maximum torque generation, five different cases, as illustrated in Figure 8, were analyzed under open loop operation with 150 V supply. From measuring the speed, it is found that, the third case with 23° conductions (-2° advance angle commutation to 21°) is proved to have the maximum positive torque for same voltage. This is very close to the conduction window obtained from the simulation results.
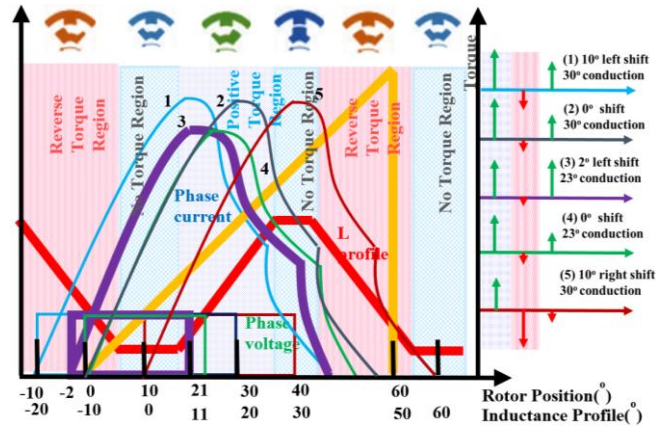
Figure 8. Conduction window analysis for maximum T_e

4. DEVELOPMENT OF ANN CONTROLLER

Using real-time training data collected from the PI speed controller, an ANN controller has been developed. For the study, PI controller is chosen as the controller for data collection due to its well-established performance in linear control applications and its ease of implementation in real-time platforms like MATLAB/Simulink [7]. Though proportional integral and derivative (PID) controllers are also a good option, in real-time embedded systems, the derivative term can introduce instability due to sampling errors. The PI controller on the other hand, gives stable and consistent responses for generating training data. However, as ANN can better handle nonlinearities and changing conditions with higher accuracy and robustness, PI controller is replaced by ANN control in the proposed study.

4.1. Implementation of PI based speed control in SRM

The speed control is obtained in the closed loop operation by changing the turn on angle using the control output from PI controller [35], [36]. MATLAB implementation of closed loop logic is as shown in Figure 9. The MATLAB blocks used for hardware deployment of the above control is as shown in Figure 10. The ramp position count obtained from the eQEP block is processed properly with respect to the inductance profile as well as index position to generate 360° position signals. The gate pulses are generated according to the commutation logic. The turn off angle is fixed at 23° whereas the turn on angle is regulated to get the set speed with in the desired conduction window with PI controller. The gate pulses generated are given out to the microcontroller using 8 GPIO blocks. For collecting the training data that should be used for ANN implementation, the real time reference speed, actual speed, current reference and turn on angle are collected using 'To workspace' Simulink block in MATLAB.
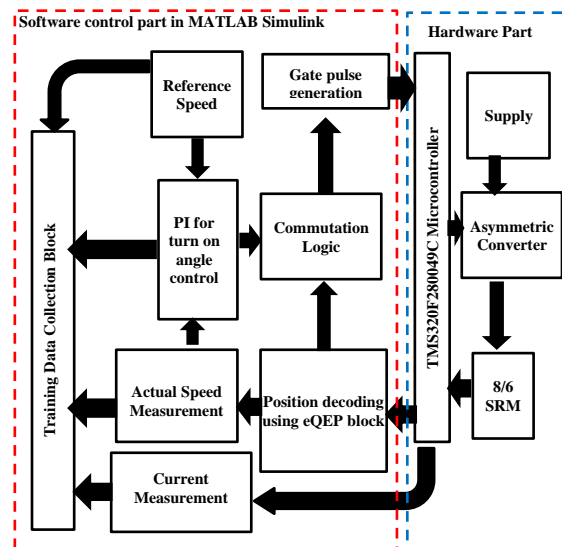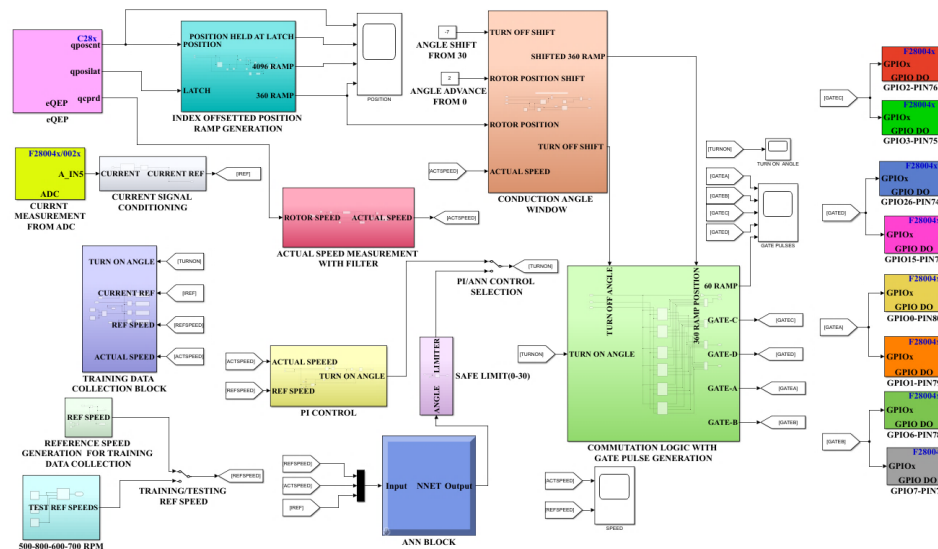

Figure 9. Closed loop operation of SRM

Figure 10. DSP interfaced MATLAB control blocks for the gate pulse generation with PI and ANN control

4.2. Implementation of ANN based speed control

The PI controller is one of the simplest and commonly used control strategies in SRM. But under considerable perturbations or system uncertainties, the response can be sluggish or overshoot may occur. This can be overcome by a competitive ANN controller which uses machine learning techniques to map the complex nonlinear relationship between input and output variables. ANN controllers can be designed to learn and adapt to changing operating conditions, making them robust to parameter variations and disturbances. They have faster dynamic response, reduced overshoot, and better steady-state performance compared to PI controllers [36]. Considering the advantages of both techniques, an ANN controller is implemented which is trained using the data obtained from the PI control. A Simulink ANN block is developed with the net fitting application which is implemented as shown in Figure 11 [37]. The performance measures such as regression coefficient (R Value), error histogram and mean squared error (MSE) are depicted in Figures 12(a)-12(c) respectively. The developed ANN model achieved an MSE of 0.004729, indicating reasonably good accuracy. In the closed- loop control as shown in Figure 10, the ANN block trained with reference speed, actual speed, and current reference as inputs and turn on angle as output is used to replace the PI block.
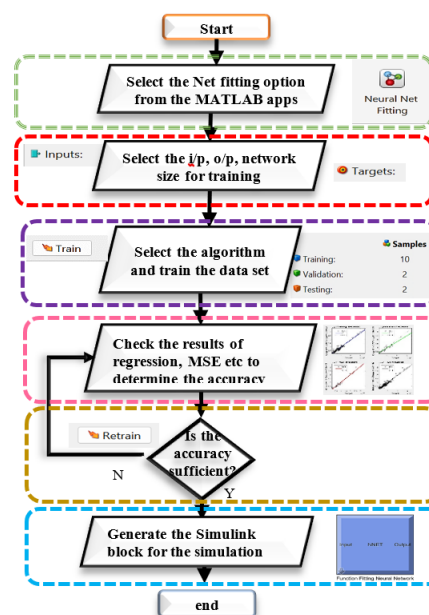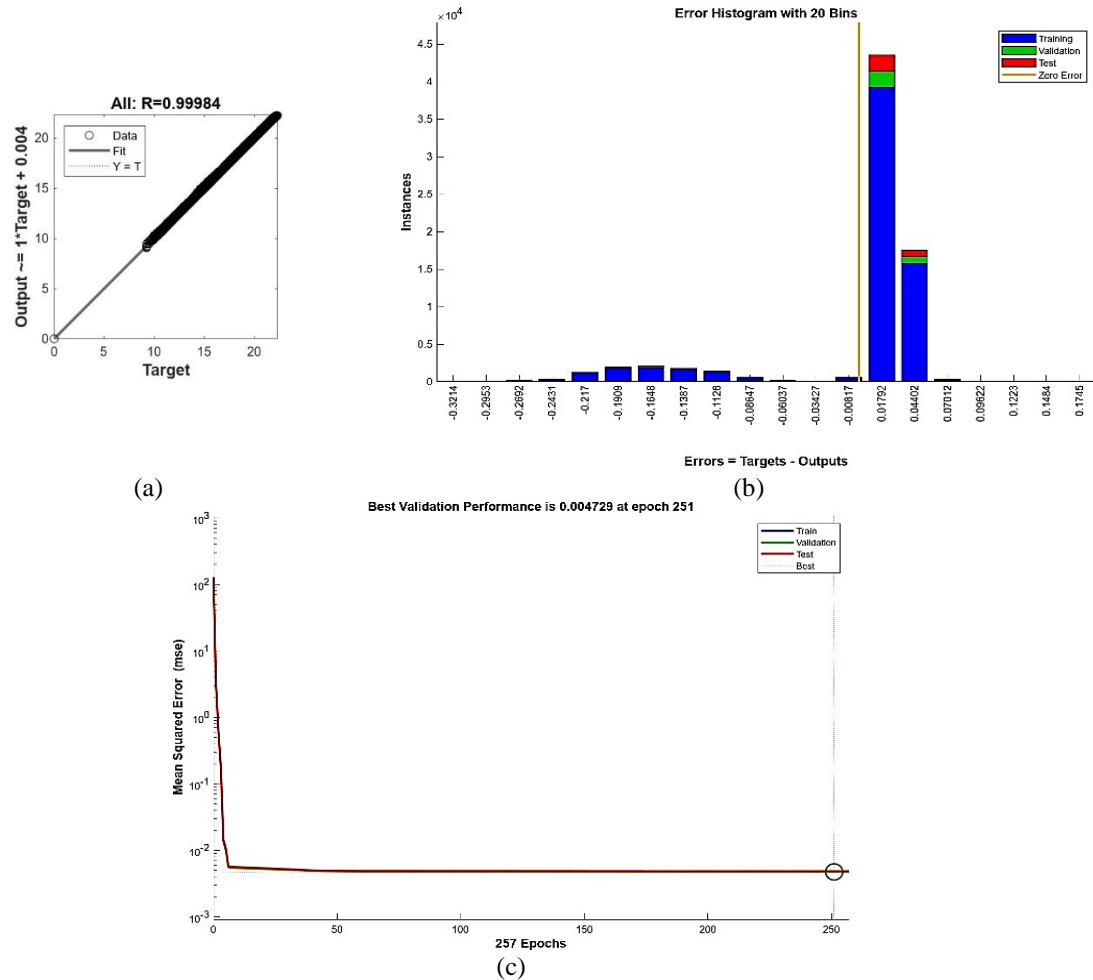

Figure 11. Flowchart for implementing ANN

(a)   (b)

(c)

Figure 12. Performance evaluation of trained ANN: (a) R-value, (b) error histogram, and (c) MSE

5.   EXPERIMENTAL IMPLEMENTATION: EVALUATIONS AND DISCUSSION

The controller's effectiveness is evaluated experimentally on a SRM with number of phases (N_{ph}) as 4 and number of stator/rotor poles (N_s/N_r) as 8/6 as represented in Figure 13. The control logic is executed on a TI TMS320F280049C controller. The motor is loaded with a brake drum arrangement. A QEP sensor is used to obtain rotor position. A diode bridge rectifier fed by a single-phase transformer is used to provide DC power to the asymmetric half bridge converter. The gate pulses generated are given by a gate drive circuit, combining the HCPL-A3120 optocoupler and CD4050 buffer IC to achieve signal isolation and level-shifting for driving IGBTs efficiently, ensuring the electrical separation of the low control circuitry voltage from the high-voltage power circuit. The phase currents are measured using LA25 Hall effect current sensor.

For training data collection,the motor is made to run in a range of 400-1000 rpm with the intervals of 50 rpm for no load as well as loaded condition using PI controller. The P and I gains obtained from the simulation analysis is used for speed control in the hardware. The training data (the reference speed ,actual speed and corresponding turn on angle change) for different speed at no load operation using ANN logic is as shown in Figures 14(a) and 14(b).

The current reference data is also collected along with the above data. A hidden layer of 10 neurons is trained using the Levenberg-Marquardt algorithm. This data being processed and are used to' instead of develop an ANN block. The turn on angle with ANN for the test speed conditions at no load is as shown in Figure 15. The same method of data collection and training is used for the speed control at load conditions also. The voltage, current and inductance waveforms at a load of 1.8 Nm are as shown in Figure 16(a). Turn on angle variation under load condition for PI and ANN controller for test conditions is shown in Figure 16(b). As depicted in Figure 16(b), the conduction angle width is considerably increased for loaded operation compared with no load operation (Figure 15) under same speed conditions with PI controller. Comparison of turn on angle variation under load condition for PI controller and ANN controller in Figure 16(b) proves that the spiky change in turn on angle during speed change is considerably reduced by using ANN controller.

Figure 17 shows a clear comparison of the speed control between PI and ANN controller. The specifications of SRM are provided in Table 1. The performance of PI and the ANN controllers, as the speed is varied from 500 to 800, 600, and 700 rpm at time intervals of 40 s, 60 s, and 80 s respectively, clearly shows that the ANN controller outperforms the PI controller across most dynamic performance metrics as shown in Table 2.

Analyzing Table 2, at $t = 80\ s$, the rise time (T_r) shows an improvement of about 8% with ANN, which reflects quicker tracking of reference speed changes compared to PI. At $t = 60\ s$, the settling time (T_s) is reduced by nearly 77%, demonstrating ANN's ability to stabilize the drive much faster. For overshoot/undershoot time (T_{os}/T_{us}), ANN achieves reductions of approximately 45% at $t = 40\ s$ and 40% at $t = 60\ s$, ensuring smoother transient behavior. The percentage overshoot is particularly minimized, with ANN achieving nearly a 95% reduction at $t = 40\ s$, highlighting its effectiveness in avoiding large deviations in motor speed. In terms of error indices, ANN reduces the root mean square error (RMSE) taken for 4 seconds from the instant of change, by around 39% at $t = 40\ s$, while the integrated square error (ISE) also shows a considerable drop, confirming improved steady-state accuracy [38].

In addition to this, Figure 18 demonstrates the effectiveness of the control even at low speeds. Furthermore, real time motor's speed reversal at 500 rpm (changing the excitation sequence) as illustrated in Figures 19(a)–19(c), showing the changes in angle, speed, and position, successfully capture the controller's dynamic response and robustness during speed inversion. Table 3 presents a comparative study of the suggested method with exiting methods. Overall, when compared to the control methods reported in literature, despite their benefits, the proposed study is more encompassing in terms of control implementation and the dynamic performance in SRM drives.
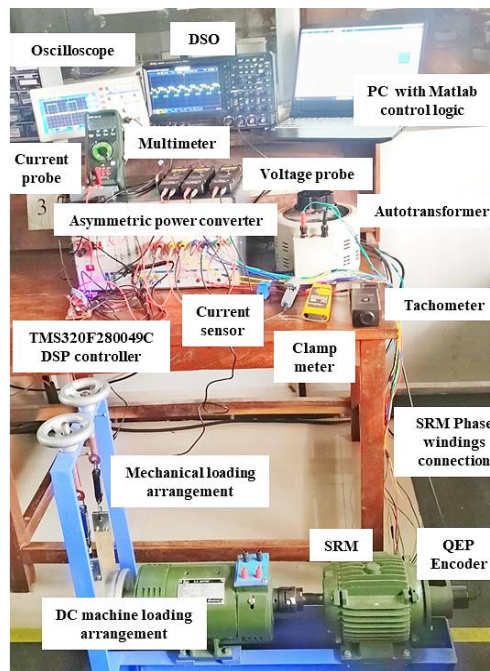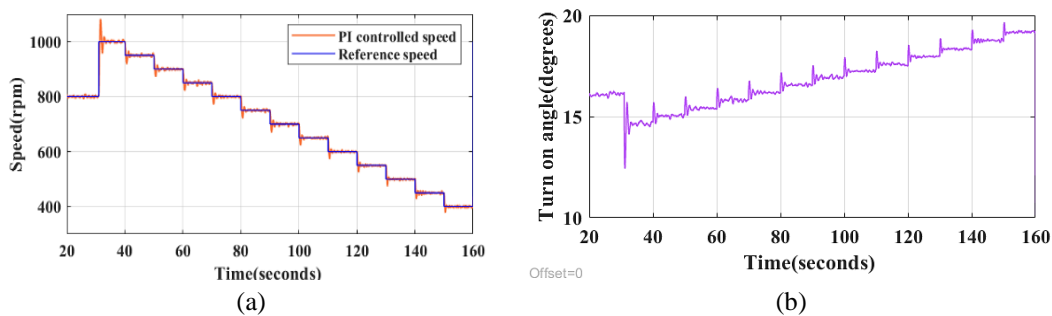

Figure 13. Hardware setup

Figure 14. Data collection process for (a) speed control and (b) turn-on angle using ANN control
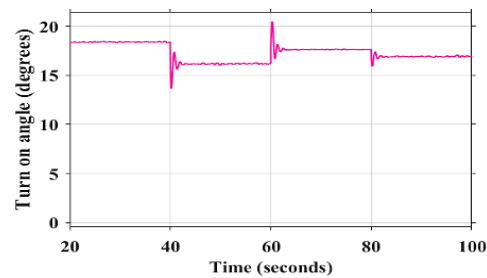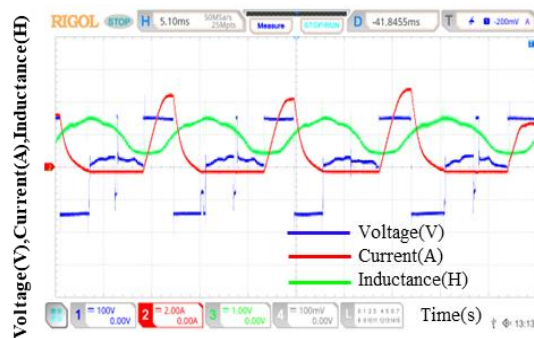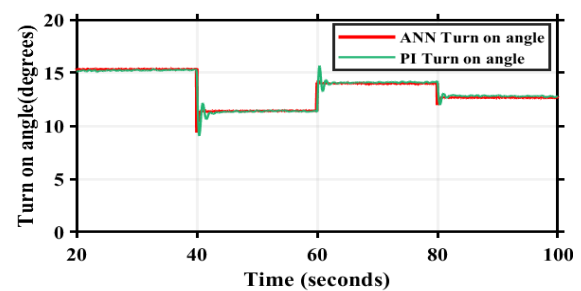
Figure 15. Turn on angle variation at no load

(a)   (b)

Figure 16. Performance validation of ANN controller under loaded condition: (a) voltage, current & inductance (x10) at 800 rpm and (b) turn on angle variation for PI and ANN controller
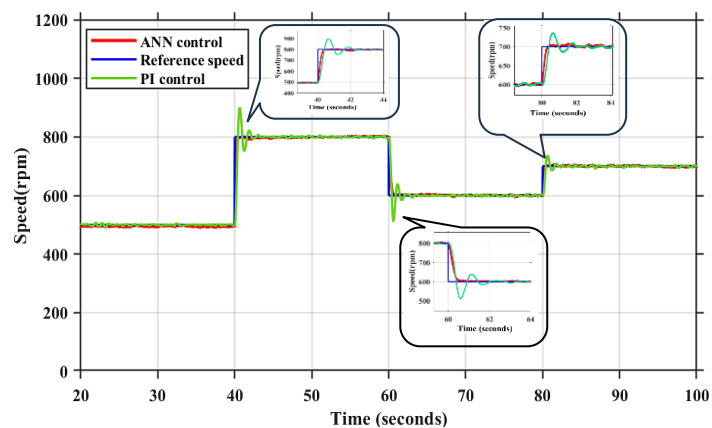

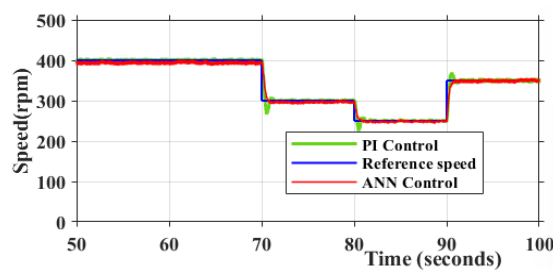Figure 17. Comparison of speed control under load condition with PI and ANN controller

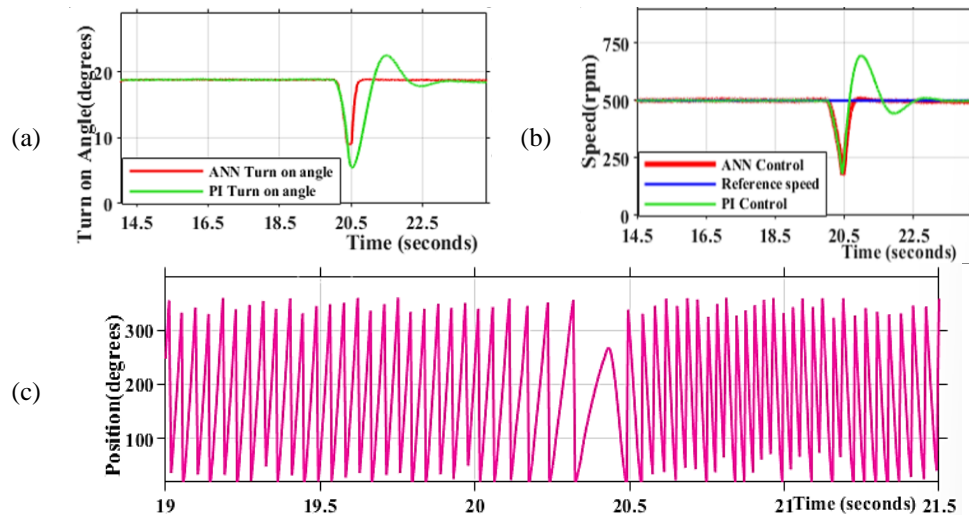Figure 18. Speed control under low speed operation

Figure 19. Speed reversal at 500 rpm: (a) turn on angle, (b) speed control, and (c) position

Table 1. SRM parameters

Parameters	Values	Parameters	Values
N_{ph}	4	R	5.6 Ω
N_s/N_r	8/6	L_u/L_a	51/194 mH
Power	500 W	Base speed	800 rpm
Voltage	150 V	B	0.0012 Nms
Current	4 A	J	0.00096 kgm^2

Table 2. Comparison of PI & ANN control

Time t(sec)	$t = 40$		$t = 60$		$t = 80$	
control	PI	ANN	PI	ANN	PI	ANN
T_r/T_f (sec)	0.41	0.39	0.38	0.38	0.37	0.34
T_s(sec)	2.50	0.6	3.00	0.70	2.1	0.5
T_{os}/T_{us}(sec)	0.92	0.51	0.70	0.42	0.74	0.39
N_{os}/N_{us} (%)	12.50	0.63	13.33	0.00	5.29	0.57
RMSE (rpm)	69.67	42.66	51.4	38.44	25.38	15.74
ISE (rpm)	2.07e^5	8.53e^4	10.71e^5	5.91e^4	2.57e^4	9.87e^3

Table 3. Comparison of existing SRM control methods and scope of proposed study

Ref.	Control method	Dynamic performance and implementation	Scope of proposed study with the literature
[5]	Fuzzy control	Moderate improvement compared with PI in simulation	Better performance especially in Ts under experimental dynamic speed conditions
[6]	Finite-time proportional control	Good transient behavior except overshoot in simulation	Smaller overshoot with practical controller deployment
[7]	Improved dynamics proportional integral control	Moderate improvement compared with PI and NN controller in simulation.	Better dynamic response verified with hardware study
[8]	Adaptive supervisory self-learning control	Good dynamic response but with complex implementation	Simplified competitive controller implementation while maintaining good dynamics
[9]	Feedforward-trained ANN control	A significant T_s in hardware experiment	Provides real-time closed-loop control with less T_s
[10]	Digital control	Good response but with high T_s, implemented with complex DSP coding	Easy beginner hardware interface, no coding needed
[11]	Fuzzy-logic robust speed control	Improved performance only in steady state error compared to PI	Improved across all metrics with full hardware validation

5. CONCLUSION

This paper comprehensively presents a detailed, step-by-step methodology for the hardware operational setup of a switched reluctance motor, providing a valuable resource for beginner researchers. The introduction of a simplified yet precise control environment, utilizing the MATLAB/Simulink platform, significantly reduces the complexity of traditional coding practices, enabling seamless implementation of control strategies. Real-time speed measurement within the MATLAB control environment ensures precise speed regulation, while the comprehensive procedure for developing the ANN block, including training data generation, offers a robust framework for implementing advanced control techniques. Furthermore, the comparative analysis of closed-loop speed control using PI and ANN techniques highlights the advantages and limitations of each approach.

AUTHOR CONTRIBUTIONS STATEMENT

This journal uses the Contributor Roles Taxonomy (CRediT) to recognize individual author contributions, reduce authorship disputes, and facilitate collaboration.

Name of Author	C	M	So	Va	Fo	I	R	D	O	E	Vi	Su	P	Fu
Veena Wilson	✓	✓	✓	✓	✓	✓		✓	✓	✓			✓	
Latha Padinjaredath Govindan				✓		✓				✓	✓	✓		✓

CONFLICT OF INTEREST STATEMENT

The absence of any conflicts of interest is confirmed by the authors.

DATA AVAILABILITY

The corresponding author, [VW], will make the supporting data available upon reasonable request.

REFERENCES

[1] N. Ali and M. Narimani, "Fault-tolerant srm drives—a review," *IEEE Transactions on Power Electronics*, vol. 39, no. 8, pp. 10261–10275, Aug. 2024, doi: 10.1109/TPEL.2024.3392713.

[2] J. W. Ahn and G. F. Lukman, "Switched reluctance motor: research trends and overview," *CES Transactions on Electrical Machines and Systems*, vol. 2, no. 4, pp. 339–347, Dec. 2018, doi: 10.30941/CESTEMS.2018.00043.

[3] E. Bostanci, M. Moallem, A. Parsapour, and B. Fahimi, "Opportunities and challenges of switched reluctance motor drives for electric propulsion: a comparative study," *IEEE Transactions on Transportation Electrification*, vol. 3, no. 1, pp. 58–75, Mar. 2017, doi: 10.1109/TTE.2017.2649883.

[4] V. Wilson and P. Latha, "Review on solutions to acoustic noise problems in switched reluctance motor using radial force improvement with two stage commutation for ev applications," *International Review of Electrical Engineering (IREE),* vol. 17, no. 2, pp. 164–176, 2022, doi: 10.15866/iree.v17i2.21379.

[5] G. Jegadeeswari, G. Ezhilarasi, V. Pramila, J. Vijayanand, and B. Kirubadurai, "Performance comparison of dynamic responses and speed control of switched reluctance motor using pi and fuzzy logic controller," in *Proceedings of the 9th International Conference on Electrical Energy Systems (ICEES), Chennai, India*, 2023, pp. 674–680, doi: 10.1109/ICEES57979.2023.10110237.

[6] Q. Yin, Z. Tian, and S. Li, "Non-smooth speed control of switched reluctance motor based on generalized proportional integral observer," in *Proceedings of the 42nd Chinese Control Conference (CCC), Tianjin, China*, 2023, pp. 3061–3066, doi: 10.23919/CCC58697.2023.10240211.

[7] G. A. A. Aziz, M. Salem, O. M. Arafa, and M. Amin, "Improved dynamics proportional-integral control of four-phase 8/6 switched reluctance motor," in *Proceedings of the 6th International Conference on Advanced Control Circuits and Systems (ACCS) and the 5th International Conference on New Paradigms in Electronics and Information Technology (PEIT), Hurgada, Egypt*, 2019, pp. 44–49, doi: 10.1109/ACCS-PEIT48329.2019.9062850.

[8] P. Saiteja, B. Ashok, B. Mason, and S. Krishna, "Development of efficient energy management strategy to mitigate speed and torque ripples in SR motor through adaptive supervisory self-learning technique for electric vehicles," *IEEE Access*, vol. 11, pp. 96460–96484, 2023, doi: 10.1109/ACCESS.2023.3311851.

[9] A. Murugesan and R. Jeyabharath, "Performance analysis and speed regulation estimation of SR motor using Ft-Ann controller with steady-state stability and FFT analysis," *Middle-East Journal of Scientific Research*, vol. 24, no. 12, pp. 3667–3677, 2016.

[10] T. F. Ali, D. A. Dominic, and P. Prabhakaran, "A systematic approach to digital control development for four-phase SRM drive using single current sensor for medium power applications," *IEEE Access*, vol. 12, pp. 34074–88, 2024, doi: 10.1109/ACCESS.2024.3372988.

[11] Z. Omaç, "Fuzzy-logic-based robust speed control of switched reluctance motor for low and high speeds," *Turkish Journal of Electrical Engineering and Computer Sciences*, vol. 27, pp. 316–329, 2019, doi: 10.3906/elk-1712-186.

[12] A. Uysal and R. Bayir, "Design and implementation of switched reluctance motor driver for industrial controller," in *Proceedings of the 4th International Conference on Power Engineering, Energy and Electrical Drives, Istanbul, Turkey*, 2013, pp. 770–774. doi: 10.1109/PowerEng.2013.6635707.

[13] A. K. Rana and A. V. R. Teja, "A fault-tolerant power converter with multi-switch fault diagnosis and repair capability for 4-phase 8/6 SRM drives," *IEEE Transactions on Transportation Electrification*, vol. 8, no. 3, pp. 3896–3906, Sep. 2022, doi: 10.1109/TTE.2022.3161090.

[14] Y. Xu and Y. Zhang, "The design of controller for SRM based on STM32," in *Proceedings of the IEEE 3rd Information Technology, Networking, Electronic and Automation Control Conference (ITNEC), Chengdu, China*, 2019, pp. 1692–1696. doi: 10.1109/ITNEC.2019.8729274.

[15] Y. Xiao, L. Shi, P. Liu, F. Han, and W. Liu, "Design of an embedded rapier loom controller and a control strategy based on SRM," *IEEE Access*, vol. 10, pp. 21914–21928, 2022, doi: 10.1109/ACCESS.2022.3153066.

[16] S. Lopez-Blandon, S. Pulgarin-Correa, and E. Giraldo, "Adaptive state space embedded control of a synchronous buck converter," in *Proceedings of the IEEE 6th Colombian Conference on Automatic Control (CCAC)*, 2023, pp. 1–6.

[17] M. Metry and R. S. Balog, "An adaptive model predictive controller for current sensorless MPPT in PV systems," *IEEE Open Journal of Power Electronics*, vol. 1, pp. 445–455, 2020, doi: 10.1109/OJPEL.2020.3026775.

[18] A. E. T. Maamar, M. Helaimi, R. Taleb, M. Kermadi, and S. Mekhilef, "A neural network-based selective harmonic elimination scheme for five-level inverter," *International Journal of Circuit Theory and Applications*, vol. 50, no. 1, pp. 298–316, Jan. 2022, doi: 10.1002/cta.3130.

[19] V. K. Awaar, N. Anjali, M. S. Rani, S. Bannuru, S. Tangallapally, and A. Siri, "Parameter estimation and speed control of foc based pmsm drive using f28379d," in *Proceedings of the IEEE 2nd International Conference on Sustainable Energy Future in Electrical Transportation (SeFeT)*, 2022, pp. 1–6.

[20] J. C. Travieso-Torres, S. S. Lee, A. Veliz-Tejo, F. Leiva-Silva, and A. Ricaldi-Morales, "Self-commissioning parameter estimation algorithm for loaded induction motors," *IEEE Transactions on Industrial Electronics*, vol. 71, no. 11, pp. 13890–13900, Nov. 2024, doi: 10.1109/TIE.2024.3357900.

[21] U. Sarkar and P. Mishra, "Indigenous design and development of interface board for tms320f28335 dsp and programming via MATLAB Simulink embedded coder," in *Proceedings of the 2025 IEEE 1st International Conference on Smart and Sustainable Developments in Electrical Engineering (SSDEE)*, Dhanbad, India, 2025, pp. 1–6. doi: 10.1109/SSDEE64538.2025.10968069.

[22] A. Elrajoubi, S. S. Ang, and A. Abushaiba, "TMS320F28335 dsp programming using matlab simulink embedded coder: techniques and advancements," in *Proceedings of the IEEE 18th Workshop on Control and Modeling for Power Electronics (COMPEL)*, Stanford, CA, USA, 2017, pp. 1–7. doi: 10.1109/COMPEL.2017.8013418.

[23] A. Fekik and others, "Hardware implementation of a solar-powered buck-boost converter for enhanced cathodic protection using texas instruments c2000 board," *IEEE Access*, vol. 12, pp. 74831–74842, 2024, doi: 10.1109/ACCESS.2024.3403207.

[24] M. A. Rahman, A. A. Abushaiba, and A. M. Elrajoubi, "Integration of c2000 microcontrollers with matlab simulink embedded coder: a real-time control application," in *Proceedings of the IEEE 7th International Conference on Electrical Engineering and Green Energy (CEEGE)*, Los Angeles, CA, USA, 2024, pp. 131–136. doi: 10.1109/CEEGE62093.2024.10744177.

[25] V. F. Pires, A. Cordeiro, D. Foito, A. J. Pires, J. Martins, and H. Chen, "A multilevel fault-tolerant power converter for a switched reluctance machine drive," *IEEE Access*, vol. 8, pp. 21917–21931, 2020.

[26] Q. Sun, J. Wu, C. Gan, and J. Guo, "Modular full-bridge converter for three-phase switched reluctance motors with integrated fault-tolerance capability," *IEEE Transactions on Power Electronics*, vol. 34, no. 3, pp. 2622–2634, 2018.

[27] P. Kumar, M. Israyelu, and S. Sashidhar, "A simple four-phase switched reluctance motor drive for ceiling fan applications," *IEEE Access*, vol. 11, pp. 7021–7030, 2023, doi: 10.1109/ACCESS.2023.3238068.

[28] T. Faheemali, D. A. Dominic, and P. Prajof, "A novel single-pulse operated SRM drive with improved performance and integrated on-board charging capability for EVs," in *2022 IEEE International Power and Renewable Energy Conference (IPRECON)*, IEEE, Dec. 2022, pp. 1–6. doi: 10.1109/IPRECON55716.2022.10059566.

[29] S.-C. Wang and W.-H. Lan, "Turn-on angle searching strategy for optimized efficiency drive of switched reluctance motors," in *Proceedings of the 30th Annual Conference of the IEEE Industrial Electronics Society (IECON)*, Busan, Korea, 2004, pp. 1873–1878. doi: 10.1109/IECON.2004.1431869.

[30] K. Manaswi, N. Jose, S. Bhaktha, B. Venkatesaperumal, and K. V Gangadharan, "Implementation of PWM speed control for SRM drive using tms320f28069 microcontroller," in *Proceedings of the IEEE 1st International Conference on Cyber Physical Systems, Power Electronics and Electric Vehicles (ICPEEV)*, Hyderabad, India, 2023, pp. 1–6. doi: 10.1109/ICPEEV58650.2023.10391895.

[31] Texas Instruments, "TMS320F280049C – 32-bit c28x real-time microcontroller." 2025. Accessed: May. 26, 2025. [Online]. Available: https://www.ti.com/product/TMS320F280049C

[32] Texas Instruments Inc., "The essential guide for developing with c2000 real-time microcontrollers, rev. f." 2023. Accessed: May. 26, 2025. [Online]. Available: https://www.ti.com/lit/ug/sprui33f/sprui33f.pdf

[33] MathWorks, "Getting started with texas instruments c2000 microcontroller blockset – matlab \& simulink." 2024. Accessed: May. 26, 2025. [Online]. Available: https://www.mathworks.com/help/ti-c2000/ug/getting-started-withC2000-example.html

[34] Texas Instruments, *"Interfacing Quadrature Encoders Using the High-End Timer on Hercules MCUs,"* Application Report, 2015. Accessed: May. 26, 2025. [Online]. Available: https://www.ti.com/lit/an/spna228/spna228.pdf.

[35] V. Wilson, L. P. G., and V. K., "Improved two stage commutation for effective vibration reduction in switched reluctance motor using particle swarm optimization," in *Proceedings of the IEEE International Conference on Power Electronics, Smart Grid and Renewable Energy (PESGRE)*, Trivandrum, India, 2022, pp. 1–6. doi: 10.1109/PESGRE52268.2022.9715957.

[36] R. M. Bhausaheb, "Speed control of srm for hybrid electric vehicle using artificial intelligence," in *Proceedings of the IEEE 12th International Conference on Computer Communication and Network Technologies (ICCCNT)*, Kharagpur, India, 2021, pp. 1–5. doi: 10.1109/ICCCNT51525.2021.9579857.

[37] L. Szamel and M. Hamouda, "Optimum control parameters of switched reluctance motor for torque production improvement over the entire speed range," *Acta Polytechnica Hungarica*, vol. 16, no. 3, pp. 20–30, 2019, doi: 10.12700/APH.16.3.2019.3.5.

[38] M. M. A. Rahman, M. Aryal, and R. Amatya, "Speed control of dc motors using an artificial neural network (ANN)," in *Proceedings of the IEEE International Conference on Electro Information Technology (eIT)*, Eau Claire, WI, USA, 2024, pp. 333–336. doi: 10.1109/eIT60633.2024.10609891.

BIOGRAPHIES OF AUTHORS

Veena Wilson 🆔 Ⓖ SC ◯ earned her engineering undergraduate degree (in EEE) from Mahatma Gandhi University, Kerala India, and obtained her masters with specialization in electrical machines from CET, Thiruvananthapuram, Kerala, India. She is serving as an assistant professor as an Assistant Professor at FISAT, Kerala, India, and she has a total 12 years of teaching experience. She is pursuing her Ph.D. at CUSAT, Kochi, India. Her research focuses on areas such as drive systems, special electric machines, and development of electric vehicle technologies. She is reachable via email at veenawilson@cusat.ac.in.

Latha Padinjaredath Govindan 🆔 Ⓖ SC ◯ earned her engineering undergraduate degree (in EEE) from Calicut University, Kerala India, and obtained her masters with specialization in Energetics from National Institute of Technology, Calicut, Kerala, India. She was awarded her Ph.D. from CUSAT, Kochi, India. She is serving as an associate professor at CUSAT, Kochi, India. She possesses over 30 years of teaching experience and now holds the position of the Head of the EEE department, CUSAT. Her research focuses on areas such as power systems, power quality, electric vehicles, and machine learning. She can be contacted at email: pglatha@cusat.ac.in.